



Population balance model and calibration method for simulating the time evolution of floc size distribution of activated sludge flocculation

Zhenliang Li^{a,b}, Daijun Zhang^{c,d,*}, Peili Lu^{c,d}, Gangcai Chen^{a,b}, Hongqiang Jiang^e

^aCollege of Urban Construction and Environmental Engineering, Chongqing University, Chongqing 400044, China, emails: zhenliangli@163.com (Z. Li), chenggangcai66@163.com (G. Chen)

^bChongqing Research Academy of Environmental Sciences, Chongqing 401147, China

^cState Key Laboratory of Coal Mine Disaster Dynamics and Control, Chongqing University, Chongqing 400044, China, emails: dzhang@cqu.edu.cn (D. Zhang), lupl@cqu.edu.cn (P. Lu)

^dDepartment of Environmental Science, Chongqing University, Chongqing 400044, China

^eState Environmental Protection Key Laboratory of Environmental Planning and Policy Simulation, Beijing 100011, China, email: jianghq@caep.org.cn

Received 8 June 2016; Accepted 24 October 2016

ABSTRACT

A population balance model (PBM) was developed to simulate the time evolution of floc size distribution (FSD) during flocculation of activated sludge. A binomial breakage function was applied to describe the daughter-particle distribution, and a fractal scaling relationship between the maximum and equivalent diameters of floc was integrated into the expressions for collision frequency and breakage frequency. The introduction of the ratio of breakage rate coefficient to collision efficiency and a two-step calibration method could simplify parameters calibration: first, the ratio of breakage rate coefficient to collision efficiency was estimated from the steady-state FSD, and then collision efficiency was obtained from the time evolution of FSD during flocculation. The results show that: (1) the time evolution of FSD during flocculation process of activated sludge can be simulated successfully by PBM; (2) fitting volume percentage and fitting mean size could give better simulation to FSDs and mean size, respectively; (3) collision efficiency and breakage rate coefficient both show power-law relationship with velocity gradient, and the former decreases while the latter increases with rise of velocity gradient; and (4) FSD simulated by using binomial distribution gives better agreement with experimental data than that simulated by using binary distribution. These results contribute to a better understanding of application of PBM on flocculation dynamics of activated sludge.

Keywords: Population balance model; Floc size distribution; Flocculation; Activated sludge; Parameters calibration; Binomial distribution

1. Introduction

Activated sludge process is one of the most popular processes used for biological wastewater treatment. In this process, bioflocs are formed in aeration tanks and separated from effluent in secondary sedimentation tank. The understanding on flocculation dynamics of activated sludge is beneficial to design and operation of separation unit [1].

The mathematical modeling of flocculation process usually makes use of the population balance model (PBM), in which the dynamics are simulated by the change in floc size distribution (FSD) that induced by simultaneous aggregation and breakage [2,3]. Generally, models only predicted the change in mean size of flocs and the final FSD at steady state when aggregation and breakage counterbalanced each other [4–8]. Moreover, discrepancies between the predicted and measured results have always been observed, and it is very difficult to obtain the time evolution of FSD during flocculation [9–11]. Different from shear-induced flocculation

* Corresponding author.

of inorganic particles, the flocculation of activated sludge is effected by various factors, including the floc's physical-chemical characteristics and external environmental conditions, such as dissolved oxygen concentrations, pH values, etc. [12–15]. For the application of PBM in modeling flocculation process of activated sludge, the key challenge is selection or development of suitable kinetic expressions for aggregation and breakage of bioflocs [10]. Solving the inverse problem has been suggested as an alternative way to get a grip on the different expressions for aggregation of activated sludge [16–18]. These studies have provided valuable findings for where existing expressions for aggregation fail to capture the true dynamics of activated sludge flocculation.

In order to achieve a good overall description of settling performance, PBM for flocculation is mainly used by coupling the sediment transport modeling [19] or CFD model [20,21]. This makes the associated computational cost and parameters estimation should be considered in the application. Compared with parameters for describing the steady-state FSDs, which have always been estimated by fitting on the volume percentage distribution or mean size at steady state, parameters for the time evolution of FSDs are more difficult to obtain [11]. As a consequence, it is necessary to find a simplified estimation method for these parameters to reduce computational cost for the application of PBM.

The aim of this work is to establish a PBM-based method to accurately simulate the time evolution of FSD in flocculation process of activated sludge. A binominal function was applied to describe the distribution of daughter particles generated from floc breakage, and the fractal dimension of activate sludge was coupled in the models for aggregation and breakage. A simplified two-step method of parameters calibration was proposed: first, the ratio of breakage rate coefficient to collision efficiency was obtained from the steady-state FSD, and then collision efficiency was obtained from the time evolution of FSD during flocculation.

2. Materials and methods

2.1. Experimental section

Flocculation experiments were conducted in mixing tank (ZR4-6, China) using aerobic activated sludge collected from municipal wastewater treatment plant. The volume of mixed liquid in tank is 1 L and concentration is 0.1 kgSS m⁻³. By adjusting the stirring speed (80–280 r·min⁻¹), average velocity gradient (G) was set as 28.2–149.8 s⁻¹, which is in the range of velocity gradient (20–200 s⁻¹) in typical activated sludge system [4].

$$G = \left(\frac{\varepsilon}{\nu} \right)^{1/2} \quad (1)$$

Table 1
Velocity gradients in mixing tank and laser particle size analyzer used in experiments

Mixing tank	Stirring speed (r·min ⁻¹)	80	150	210	280	550
	G (s ⁻¹)	28.2	64.7	101.7	149.8	360.3
Laser particle size analyzer	Injection flow (mL·s ⁻¹)	6.5	13	19.5	29.25	65
	G (s ⁻¹)	33.1	66.2	99.3	149.0	331.0

where ε represents the homogeneous turbulent energy dissipation rate of mixed tank and ν is the kinematic viscosity of suspending fluid.

The FSDs of activated sludge during flocculation were measured using laser particle size analyzer (S3500, Microtrac). After being introduced into injection port, flocs flowed through the sampling pipe (length = 40 cm and inner diameter = 1 cm) to optical measuring system. By controlling suitable sample flow rates, velocity gradients in sampling pipe were kept close to that in mixing tank to reduce the possible effect on FSD due to the difference of flowing shear (Table 1). The initial FSD of activated sludge was generated by mechanical breakage at stirring speed of 550 r·min⁻¹. This speed corresponds to the maximum velocity gradient of 360.3 s⁻¹ that could be reached in sampling pipe of laser particle size analyzer.

Two-dimensional fractal dimension D_2 of activated sludge was determined based on microscopy and image analysis [22]. Flocs were placed into Petri dishes and diluted with deionized water. The computerized microscope (XPV-600E, China) was used to take pictures. After binary processing of these pictures, pixel numbers of equivalent diameter L_i and maximum diameter (i.e., circumscribed circle diameter) $L_c(i)$ were counted [23]. The relationship between $L_c(i)$ and L_i can be written as:

$$\left(\frac{L_c(i)}{L_p} \right)^{D_2} \approx \frac{A_i}{A_p} = \left(\frac{L_i}{L_p} \right)^2 \Rightarrow L_c(i) \approx \left(\frac{L_i}{L_p} \right)^{\frac{2}{D_2}} L_p \quad (2)$$

where L_p is the primary particle size, A_i is the area of floc in class i , and A_p is the area of primary particle.

2.2. Models

A PBM with aggregation and breakage was used to describe the rate of change of the particle number concentration as follows [24,25]:

$$\begin{aligned} \frac{dn(v,t)}{dt} = & \frac{1}{2} \int_0^v \alpha \beta(v-u) n(v-u,t) n(u,t) du - n(v,t) \\ & \int_0^\infty \alpha \beta(v,u) n(u,t) du + \\ & \int_v^\infty b(v|w) S(w) n(w,t) dw - S(v) n(v,t) \end{aligned} \quad (3)$$

where $n(v,t)$ is the number concentration of flocs of volume v , α is the collision efficiency, $\beta(v,u)$ is the collision frequency of flocs of volume v and u , $b(v|w)$ is the breakage probability density function of flocs of volume w into flocs of volume v , and $S(w)$ is the breakage rate for flocs with volume of w .

The first term on right-hand side of Eq. (3) represents the production rate of flocs with volume v due to aggregation between flocs of volume $v - u$ and u . The second term denotes the loss of flocs with volume v due to its aggregation with the rest of flocs. The third term on the right describes the production rate of flocs with volume v when larger flocs with volume w break into particles with volume v . The fourth term is the loss of flocs when it breaks into smaller flocs.

Following the fixed pivot technique [26], the discretized population balance for the change in number of flocs N_i in class i is given by the following expression:

$$\frac{dN_i}{dt} = \sum_{\substack{j,k \\ v_{i-1} \leq (v_j+v_k) \leq v_{i+1}}}^{j \geq k} \left[1 - \frac{1}{2} \delta_{j,k} \right] \eta_i \alpha \beta(j,k) N_j N_k - N_i \sum_k \alpha \beta(i,k) N_k + \sum_{j \geq i} \gamma_{j,i} S(j) N_j - S(i) N_i \quad (4)$$

where $\delta_{j,k}$ is Dirac delta function, $\gamma_{j,i}$ is the breakage distribution function defining the fraction of a daughter particle of class size i breaking from a floc of class size j , and η_i is a proportional coefficient assigning the fraction of the floc v_i from the aggregate $(v_j + v_k)$:

$$\eta_i = \begin{cases} \frac{v_{i+1} - (v_j + v_k)}{v_{i+1} - v_i} & v_i \leq (v_j + v_k) \leq v_{i+1} \\ \frac{(v_j + v_k) - v_{i-1}}{v_i - v_{i-1}} & v_{i-1} \leq (v_j + v_k) \leq v_i \end{cases} \quad (5)$$

Generally, collision efficiency α is considered as a constant with value of 0–1, and needs to be calibrated using experimental data [2,4]. Because floc collision and breakage occur at the same time, collision efficiency and breakage frequency coefficient can be calibrated simultaneously [19].

Collision frequency and breakage frequency due to shear rate have usually been assumed to be dependent on floc size [4,27,28]. Considering that the maximum size determines more directly the interactions between flocs [29], collision frequency and breakage rate can be calculated from:

$$\beta(i,j) = \frac{G}{6} (L_c(i) + L_c(j))^3 = \frac{G}{6} \left[\left(\frac{L_i}{L_p} \right)^{\frac{2}{D_2}} L_p + \left(\frac{L_j}{L_p} \right)^{\frac{2}{D_2}} L_p \right]^3 \quad (6)$$

and

$$S(i) = EL_c(i) = E \left(\frac{L_i}{L_p} \right)^{\frac{2}{D_2}} L_p \quad (7)$$

where E is the breakage frequency coefficient.

The mostly used functions for daughter-particle distribution are simple binary distribution and normal distribution [3,27]. When a uniform computational grid, i.e., $v_i = iv_p$ (v_p is the volume of fundamental particle), was used to solve the PBM, the normal distribution could be approximated to a binomial distribution. Therefore, $\gamma_{j,i}$ can be calculated from [28,30]:

$$\gamma_{j,i} = \binom{j}{i} / \sum_{i=1}^j \binom{j}{i} \quad (8)$$

According to Eq. (8), the higher probability of daughter-particle distribution occurs when the volume of daughter particle is close to half of original particle. However, the load of calculation on a uniform computational grid was comparatively large while the size range of flocs is wide (e.g., 5–1,000 μm). If a geometric grid with factor k ($v_i = kv_{i-1}$, $1 < k \leq 2$) was adopted to solve the PBM, a binomial distribution in another form can be used for daughter-particle distribution [31]:

$$\gamma_{j,i} = \binom{j}{i} p^i (1-p)^{j-i} \quad (i = 1, 2, \dots, j) \quad (9)$$

The shape of a binomial distribution is determined by class number j and parameter p , and the probability mass function has its peak at location $j \times p$. Defining the parameter C_p to determine the location at which probability mass function has its peak, then

$$p = (i - C_p) / i \quad (10)$$

Assuming that the daughter particles whose volume is half of original floc has the highest probability, C_p can be calculated from [31]:

$$C_p = \log(2) / \log(k) \quad (11)$$

2.3. Data transformation

The raw output of laser particle size analyzer is volume percentage (vol%) distribution for a given grid. However, PBM is formulated on number concentration basis and might use the other grids. Recalculation of the experimental data is required to make them compatible with model grid. The cumulative vol% distribution is first calculated from the raw vol% distribution, and then interpolated at the pivots of new grid resulting in the new cumulative distribution, allowing recalculation of vol% distribution. Besides, a volume-to-number conversion is needed to obtain an initial distribution to feed the model. The experimental data are expressed as vol%, i.e., the ratio of floc volume of class i (V_i) to total volume of all classes (V), V_i/V ; and PBM is expressed as number concentrations N_i or the ratio of number of particles of class i to total sample volume V_T . To convert V_i/V to N_i , the total floc volume fraction V/V_T is needed [32]:

$$N_i = \left(\frac{6}{\pi L_i^3} \right) \frac{V_i}{V_f} \frac{V_f}{V_T} \quad (12)$$

$$\frac{V_f}{V_T} = \frac{(1+C)X}{\rho_f} \quad (13)$$

where X is the mixed liquid suspended solids and ρ_f is the density of flocs. C is the ratio of liquid to solid mass within a sludge floc:

$$C = \frac{\rho_l(\rho_s - \rho_f)}{\rho_s(\rho_f - \rho_l)} \quad (14)$$

where ρ_l and ρ_s is the density of liquid and dry solids, respectively.

In this study, the total floc volume fraction for the sludge with $X = 0.1 \text{ kg}\cdot\text{m}^{-3}$, $\rho_l = 1,000 \text{ kg}\cdot\text{m}^{-3}$, $\rho_s = 1,700 \text{ kg}\cdot\text{m}^{-3}$, and $\rho_f = 1,040 \text{ kg}\cdot\text{m}^{-3}$ was found to be 0.10%.

2.4. Numerical solution

The integration method of Eq. (4) consists of computing the discrete $\Delta N_i/\Delta t$. A geometric grid with a factor of $k = 1.6$ was used, i.e., $v_i \approx 1.6 v_{i-1}$, aligning with Fibonacci series rule of $v_i + v_{i-1} \approx v_{i+1}$. Integrating Eq. (4) involved computing the discrete $\Delta N_i/\Delta t$ of dN_i/dt values. The solution equation was derived using Euler method, which involved establishing 0.1–1 s as the iterative calculation of Δt to maintain calculation stability [33]. The final state of flocculation is that floc aggregation and breakage counterbalance each other, i.e., $dN_i/dt = 0$ in Eq. (4). Connecting Eqs. (7) and (4) yield

$$\frac{dN_i}{dt} = \alpha \left\{ \sum_{\substack{j \geq k \\ v_{i-1} \leq (v_j + v_k) \leq v_{i+1}}} \left[1 - \frac{1}{2} \delta_{j,k} \right] \eta_i \beta(j,k) N_j N_k - N_i \sum_k \beta(i,k) N_k \right\} - E \left[L_c(i) N_i - \sum_{j \geq i} \gamma_{j,i} L_c(j) N_j \right] = 0 \quad (15)$$

Eq. (15) shows the correlation between breakage rate coefficient E and collision efficiency α . The number concentration of flocs in each class can be obtained when the ratio of breakage rate coefficient and collision efficiency has calibrated using the experimental data.

In this work, a two-step method of parameters calibration was proposed:

- (i) The ratio of breakage rate coefficient to collision efficiency was calibrated from the steady-state FSD. The volume percentage and mean size (L_{mean}) can be chosen as fitting variables [32], so we defined the minimum error for parameters calibration as:

$$Err_1 = \frac{1}{n} \sum_{i=1}^n |m(i) - m'(i)| \quad (16)$$

$$Err_2 = |L_{\text{mean}} - L'_{\text{mean}}| \quad (17)$$

where n is the total number of classes of flocs, and $m(i)$ and $m'(i)$ are the measured and simulated volume percentage of flocs in class i at steady state, respectively. L_{mean} and L'_{mean} are the measured and simulated mean size of flocs at steady state, respectively, and

$$L_{\text{mean}} = \frac{\sum_i L_i V_i}{\sum_i V_i} \quad (18)$$

where V_i is the total volume of floc in class i .

- (ii) Assuming that the ratio of breakage rate coefficient to collision efficiency unchanged in flocculation, collision efficiency was obtained from the time evolution of FSD. We defined the minimum error for parameters calibration as:

$$Err_3 = \frac{1}{m} \frac{1}{n} \sum_{t=t_1}^{t_m} \sum_{i=1}^n |m(t,i) - m'(t,i)| \quad (19)$$

$$Err_4 = \frac{1}{m} \sum_{t=t_1}^{t_m} |L_{\text{mean}}(t) - L'_{\text{mean}}(t)| \quad (20)$$

where $m(t,i)$ and $m'(t,i)$ are the measured and simulated volume percentage of floc in class i at time t , respectively. t_1 and t_m are the starting and ending time during flocculation process, respectively. $L_{\text{mean}}(t)$ and $L'_{\text{mean}}(t)$ are the measured and simulated volume mean floc size at time t , respectively.

The conservation of number and volume of all particles should be maintained during the numerical solution of PBM. Flocs with different sizes can be considered as the aggregations of primary particles [33]. Assuming the floc with the minimum measured size is primary particle, the total number concentrations of primary particles N_p can be obtained. We defined two indices, N_{cons} and V_{cons} , to assess the conservation of number and volume of primary particles as:

$$N_{\text{cons}} = \sum_{i=1}^n k^{i-1} N_i - N_p \approx 0 \quad (21)$$

$$V_{\text{cons}} = \sum_{i=1}^n \frac{\pi L_i^3}{6} N_i - \frac{V_f}{V_T} \approx 0 \quad (22)$$

3. Results

3.1. Steady-state FSD

The FSDs during flocculation were presented as volume percentage distributions. The fractal dimension D_2 of activated sludge floc was estimated to be 1.83 by the best fit to these measured data of $L_c(i)$ and L_i (Fig. 1).

Provided the computation time is adequate, the change rate of number concentration $dN_i/dt < 1$ could be achieved and used to detect the proximity to the steady state of flocculation. Then, the ratio of breakage rate coefficient to collision efficiency could be estimated from the measured FSD at steady state. Fig. 2 shows the average error of volume percentage distribution at steady state with different collision efficiencies α and breakage rate coefficient E . The minimum error (0.0041 or less) occurs when E is directly proportional to α . Meanwhile, the results show that N_{cons} and V_{cons} always keep approximately zero during the whole simulation time (Fig. 3), indicating that the total number and volume of primary particles remain almost unchanged.

The simulated FSDs by fitting on volume percentage and mean size are similar to the measured results under different velocity gradient (Fig. 4). Compared with the results obtained

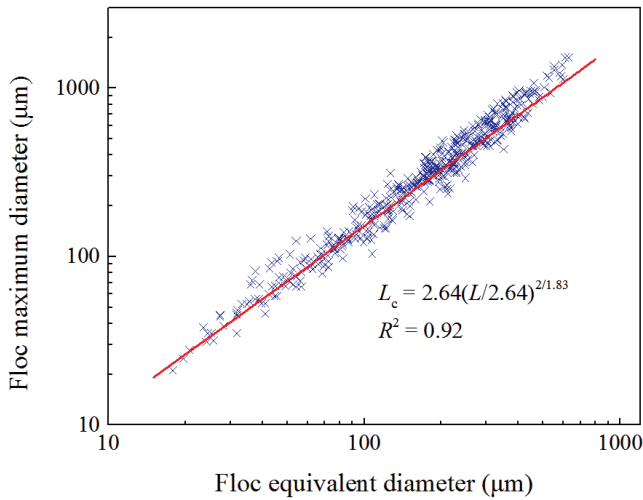


Fig. 1. Two-dimensional fractal dimension of activated sludge flocs calculated by fitting to Eq. (2) (the primary particles size L_p was approximate to the pixel size 2.64 μm).

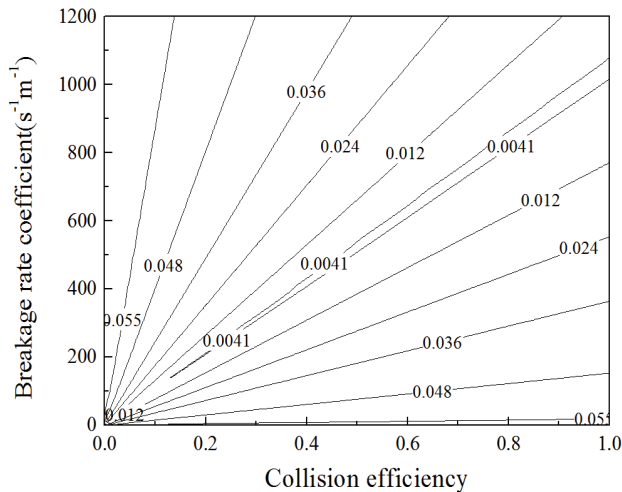


Fig. 2. Average error of volume percentage distribution with different collision efficiency α and breakage rate coefficient E for simulation of steady-state FSD under velocity gradient of 28.2 s^{-1} .

by fitting on mean size, the simulated FSDs obtained by fitting on volume percentage give better agreement to the measured results. The simulated mean sizes are less than their measurements, whereas the simulation results of mean size by fitting on mean size are nearly the same as the measured results (Table 2).

3.2. Time evolution of FSD

The ratio of breakage rate coefficient to collision efficiency, E/α , represents the relationship between floc collision and breakage. It seems related to the factors influencing the flocculation except velocity gradient, such as sludge properties and environmental conditions. In the flocculation process, the flocculation balance factor might

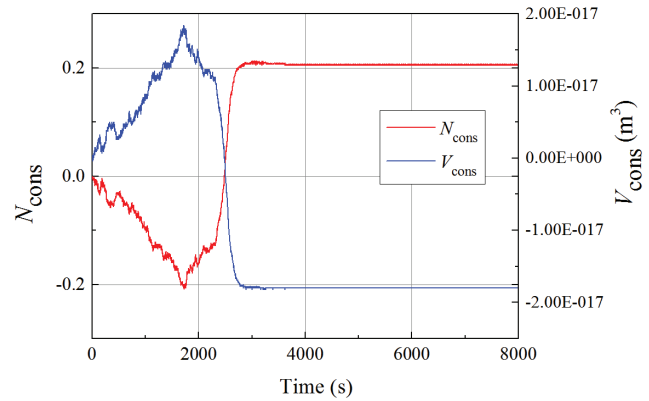


Fig. 3. Time evolution of N_{cons} and V_{cons} during simulation of FSD under velocity gradient of 28.2 s^{-1} .

not change. However, the simulated FSD during flocculation could vary with different collision efficiency α (or the value of breakage rate coefficient E). Fig. 5 shows the time evolutions of mean floc size using different values of collision efficiency.

In Fig. 5, the time evolutions of mean floc size under different velocity gradients were simulated well by using the optimum collision efficiency α_{opt} estimated by fitting on mean floc size. Similarly, the simulation results of time evolution of FSD during flocculation show a good agreement with the experiments by using the optimum collision efficiency α_{opt} estimated by fitting on volume percentage (Fig. 6). However, the results demonstrate that α_{opt} estimated by fitting on volume percentage is slightly different from that obtained by fitting on mean size.

4. Discussion

The introduction of the ratio of breakage rate coefficient to collision efficiency, E/α , is helpful to simplify the parameters calibration, and the model parameters could be estimated in two steps: first, E/α is obtained from the steady-state FSD, and then collision efficiency is estimated from the time evolution of FSD during flocculation. Thus, there is only one parameter need to be estimated in each step. Similar method for the first step was also applied by Mietta et al. [19], and the ratio of collision efficiency to breakage rate coefficient was estimated from the experimental data.

The volume percentage or mean size can be chosen as the fitting variables. The relatively more accurate results of FSDs would be obtained by fitting on the former, and the relatively more accurate results of mean size would be obtained by fitting on the latter. Theoretically, the simulated results of mean size should be more close to the measured results as long as the more accurate results of FSDs obtained. However, in this study, we found that the simulated mean sizes are less than their measurements by fitting on volume percentage (Table 2). This is mainly due to the error in simulation for volume percentage of large flocs (about $L > 200 \mu\text{m}$). Although these volume percentages of large flocs are relatively small, they make a significant contribution to the value of mean size calculated from Eq. (18).

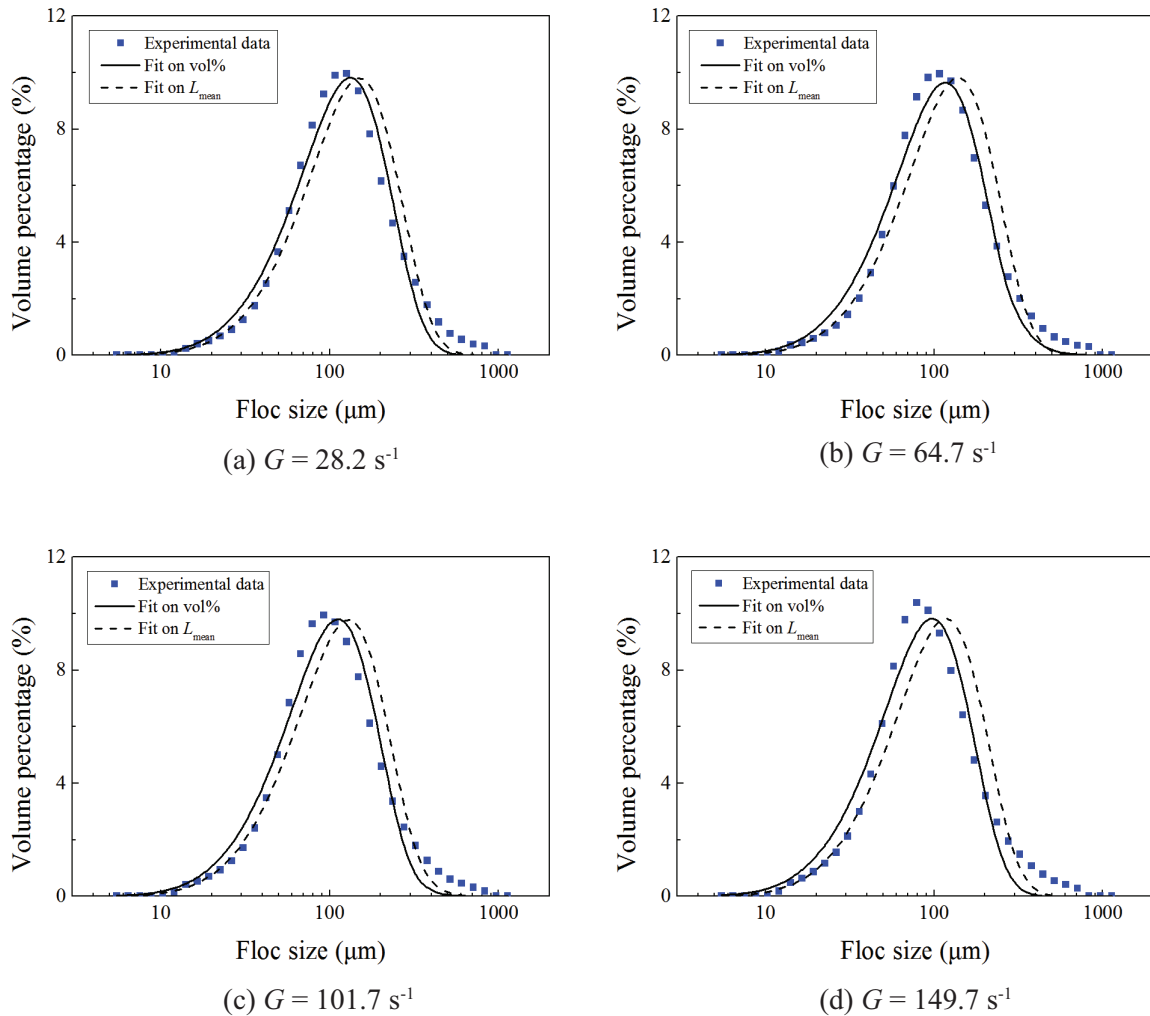


Fig. 4. Predictions of steady-state FSDs under different velocity gradients by fitting on volume percentage (vol%) and mean size (L_{mean}).

The results show that the ratio of breakage rate coefficient to collision efficiency increases with rise of velocity gradient (Table 2), whereas the optimum collision efficiency α_{opt} (Figs. 5 and 6) decreases with rise of velocity gradient. In the shell-core model proposed by Kusters et al. [34], collision efficiency shows a power-law relationship with velocity gradient. Previous studies have also found that collision efficiency decreases with increase of shear rate [4,35]. Therefore, the relationship between the optimum collision efficiency and velocity gradient can be described as:

$$\alpha_{\text{opt}} = C_1 G^{b_1} \quad (23)$$

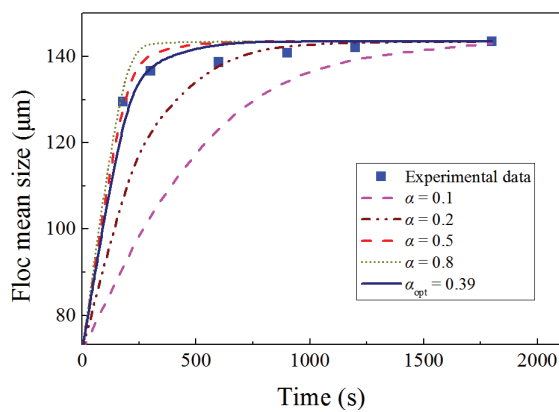
where C_1 and b_1 are constants.

The fitting results were shown in Fig. 7. The optimum breakage rate coefficient was obtained by product of the ratio of breakage rate coefficient to collision efficiency and the optimum collision efficiency. The results show that the optimum breakage rate coefficient is positively correlated to velocity gradient, which agrees to the conclusions of previous studies [4,27].

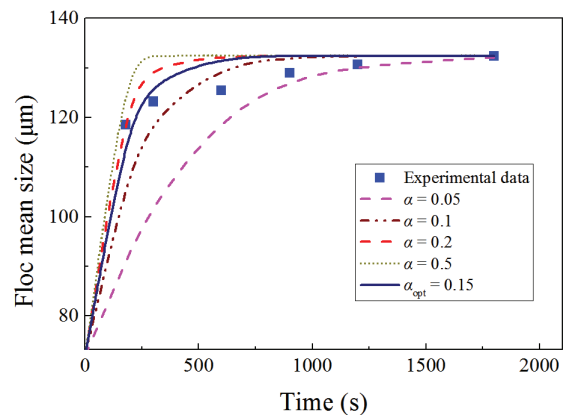
We compared the simulation results of steady-state FSD obtained by using binomial and binary breakage distribution (Fig. 8). For binary distribution, assuming the floc with volume v_i breaks up into two equal size daughter particles, the newly formed floc is represented by assigning proportional fractions to the flocs with volume v_{i-2} and v_{i-1} . The simulation results are similar to each other, which is consistent with the conclusion drawn by Zhang and Li [3]. This agreement might attribute to the fact that binomial distribution is not significantly different from binary distribution when the binomial distribution parameter C_p is calculated from Eq. (11), which would result in the highest generation probability of daughter particles whose volume equals half of original floc. However, the values of Err_1 and Err_2 obtained by using binomial distribution were less than that obtained by using binary distribution, suggesting that the simulation results of steady-state FSD and mean size by using binomial distribution give better agreement with experimental data.

Table 2
Optimum values for parameter E/α for different velocity gradients by fitting on volume percentage (vol%) and mean size (L_{mean})

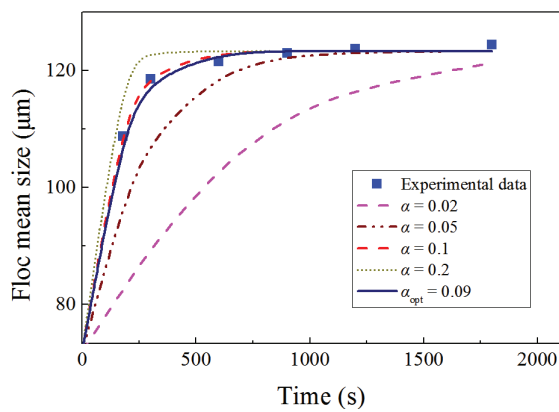
G (s^{-1})	Fitting variable	Calibrated values of parameters E/α ($\text{m}^{-1}\cdot\text{s}^{-1}$)	Average error of volume percentage Err_1	Simulated mean size (μm)	Experimental mean size (μm)
28.2	vol%	1,025	4.09×10^{-3}	126.85	143.49
	L_{mean}	927	5.62×10^{-3}	143.44	
64.7	vol%	2,611	3.90×10^{-3}	115.58	132.43
	L_{mean}	2,270	6.03×10^{-3}	132.41	
101.7	vol%	4,228	4.56×10^{-3}	107.24	124.48
	L_{mean}	3,770	6.24×10^{-3}	124.29	
149.8	vol%	7,003	5.37×10^{-3}	93.21	112.56
	L_{mean}	6,014	7.21×10^{-3}	112.39	



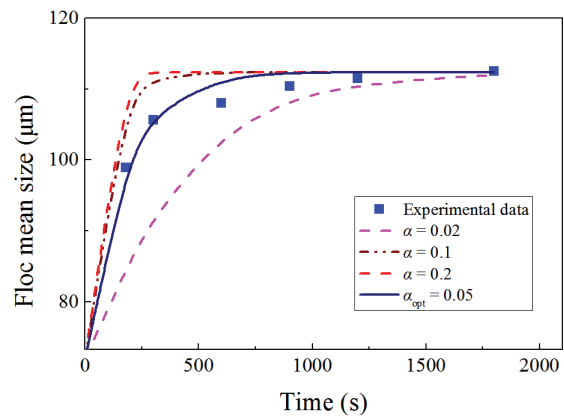
(a) $G = 28.2 \text{ s}^{-1}$



(b) $G = 64.7 \text{ s}^{-1}$



(c) $G = 101.7 \text{ s}^{-1}$



(d) $G = 149.8 \text{ s}^{-1}$

Fig. 5. Time evolution of mean floc size using different collision efficiency during flocculation under different velocity gradient (α_{opt} was optimum collision efficiency and E/α was obtained by fitting on mean size).

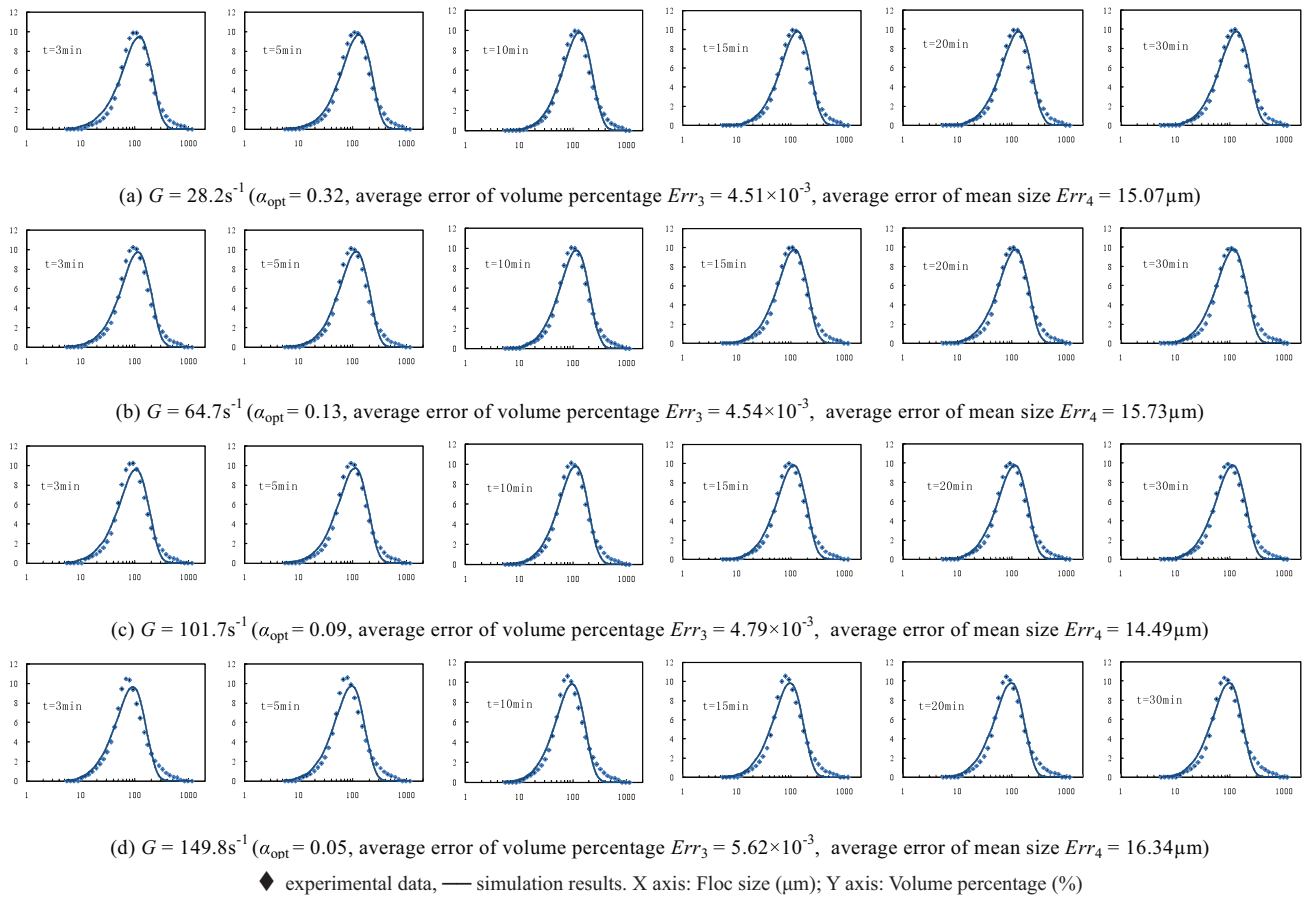


Fig. 6. Simulation results of time evolution of FSD during flocculation under different velocity gradient (α_{opt} was optimum collision efficiency and E/α was obtained by fitting on volume percentage).

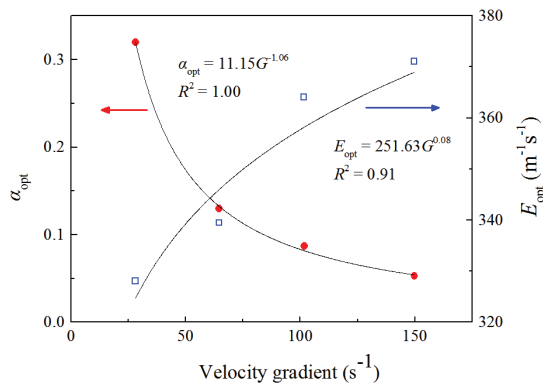


Fig. 7. Effect of velocity gradient on collision efficiency and breakage rate coefficient ($E_{opt} = E/\alpha \times \alpha_{opt}$, ratio of breakage rate coefficient to collision efficiency, E/α is obtained by fitting on vol%, and α_{opt} is optimum collision efficiency in Fig. 6).

5. Conclusions

The time evolution of FSD during flocculation process of activated sludge was simulated successfully by PBM, in which a binomial breakage function was used to describe the daughter-particle distribution and a fractal scaling relationship was

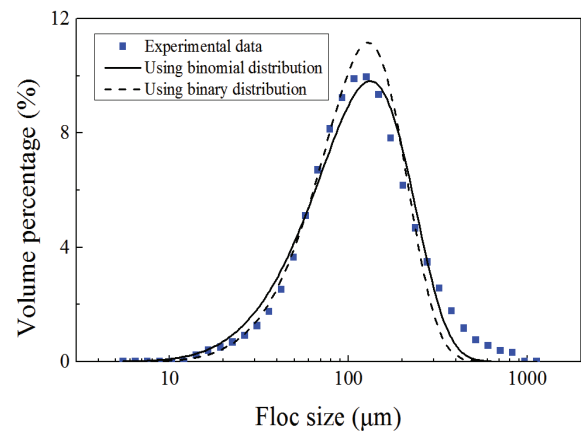


Fig. 8. Comparison of model predictions of steady-state FSD under velocity gradient of 28.2 s^{-1} by using binomial and binary distribution ($E/\alpha = 1,025 \text{ m}^{-1}\cdot\text{s}^{-1}$, $Err_1 = 4.09 \times 10^{-3}$, and $Err_2 = 16.64 \text{ μm}$ for binomial distribution, and $E/\alpha = 1,089 \text{ m}^{-1}\cdot\text{s}^{-1}$, $Err_1 = 4.42 \times 10^{-3}$, and $Err_2 = 19.21 \text{ μm}$ for binary distribution).

integrated into the expressions for collision frequency and breakage frequency. The introduction of the ratio of breakage rate coefficient to collision efficiency and a two-step

calibration method could simplify the parameters calibration. Fitting on volume percentage and mean size could give better simulation to FSDs and mean size, respectively. It is found that collision efficiency and breakage rate coefficient both show power-law relationship with velocity gradient: the former decreases while the latter increases with rise of velocity gradient; and the steady-state FSD simulated by using binomial distribution gives better agreement with the experimental data than that simulated by using binary distribution.

Acknowledgments

The work was partially supported by National Natural Science Foundation of China (51609028), Natural Science Foundation of Chongqing (CSCT2014JCYJA20001, 2015CSTC-JBKY-01605), and Scientific and Technological Research Program of Chongqing Municipal Education Commission (KJ1401406), China. The authors thank Dr. Kinza Zarin for English language editing.

Symbols

A_i	—	Area of floc in class i , m^2
A_p	—	Area of primary particle, m^2
C	—	Ratio of the liquid to solid mass within a sludge floc, see Eq. (14)
C_p	—	Binomial breakage function parameter
D_2	—	Two-dimensional fractal dimension
E	—	Breakage rate coefficient, $m^{-1}\cdot s^{-1}$
Err_1	—	Average error of volume percentage, see Eq. (16)
Err_2	—	Error of mean size, see Eq. (17)
Err_3	—	Average error of volume percentage in flocculation, see Eq. (19)
Err_4	—	Average error of mean size in flocculation, see Eq. (20)
G	—	Average velocity gradient, s^{-1}
L	—	Floc equivalent diameter or floc size, μm
L_c	—	Floc circumscribed circle diameter or maximum diameter, μm
L_{mean}	—	Mean floc size, μm
L_p	—	Primary particle size, μm
$m(i)$	—	Volume fractions of flocs in class i
n	—	Total number of classes of flocs
N_{cons}	—	Index for number conservation of primary particles, see Eq. (21)
N_i	—	Number concentration of flocs in class i , m^{-3}
p	—	See Eq. (8)
$S(i)$	—	Breakage rate of flocs in class i , s^{-1}
V_{cons}	—	Index for volume conservation of primary particles, see Eq. (22)
V_f	—	Total floc volume of all classes, m^3
v_i	—	Volume of a floc in class i , m^3
v_p	—	Volume of a fundamental particle
V_i	—	Total volume of flocs in class i , m^3
V_T	—	Total sample volume, m^3
X	—	Concentration of activated sludge, $kg\cdot m^{-3}$
<i>Greek letters</i>		
α	—	Collision efficiency
$\beta(j, k)$	—	Collision frequency between flocs of class j and k , $m^3\cdot s^{-1}$

γ_{ji}	—	Breakage distribution function
$\delta_{j,k}$	—	Dirac delta function
ε	—	Turbulent energy dissipation rate, $m^3\cdot s^{-2}$
η_i	—	Proportional coefficient, see Eq. (5)
ν	—	Kinematic viscosity, $m^2\cdot s^{-1}$
ρ_f	—	Density of flocs, $kg\cdot m^{-3}$
ρ_l	—	Density of liquid, $kg\cdot m^{-3}$
ρ_s	—	Density of dry solids, $kg\cdot m^{-3}$

References

- [1] J. Nan, W.P. He, Characteristic analysis on morphological evolution of suspended particles in water during dynamic flocculation process, *Desal. Wat. Treat.*, 41 (2012) 35–44.
- [2] D. Thomas, S. Judd, N. Fawcett, Flocculation modelling: a review, *Water Res.*, 33 (1999) 1579–1592.
- [3] J.J. Zhang, X.Y. Li, Modeling particles size distribution dynamics in a flocculation system, *AIChE J.*, 49 (2003) 1870–1882.
- [4] C.A. Biggs, P. Lant, Modelling activated sludge flocculation using population balances, *Powder Technol.*, 124 (2002) 201–211.
- [5] J. Ducoster, A two-scale PBM for modeling turbulent flocculation in water treatment processes, *Chem. Eng. Sci.*, 57 (2002) 2157–2168.
- [6] C. Coufort, D. Bouyer, A. Liné, B. Haut, Modelling of flocculation using a population balance equation, *Chem. Eng. Process.*, 46 (2007) 1264–1273.
- [7] Y.L. Yeow, J.L. Liow, Y.K. Leong, A general procedure for obtaining the evolving particle-size distribution of flocculating suspensions, *AIChE J.*, 58 (2012) 3043–3053.
- [8] J.H. Zhao, W.P. Li, X.M. Jiao, Y.P. Lai, X.Y. Guo, Floc growth kinetics in magnesium hydroxide coagulation process, *Desal. Wat. Treat.*, 52 (2014) 4334–4341.
- [9] A. Ding, M. Hounslow, C.A. Biggs, Population balance modelling of activated sludge flocculation: investigating the size dependence of aggregation, breakage and collision efficiency, *Chem. Eng. Sci.*, 61 (2006) 63–74.
- [10] I. Nopens, E. Torfs, J. Ducoste, P.A. Vanrolleghem, K.V. Gernaey, Population balance model: a useful complementary modelling framework for future WWTP modelling, *Water Sci. Technol.*, 71 (2015) 159–167.
- [11] R.I. Jeldres, F. Concha, P.G. Toledo, Population balance modelling of particle flocculation with attention to aggregate restructuring and permeability, *Adv. Colloid Interface Sci.*, 224 (2015) 62–71.
- [12] B.M. Wilén, B. Jin, P. Lant, The influence of key chemical constituents in activated sludge on surface and flocculating properties, *Water Res.*, 37 (2003) 2127–2139.
- [13] G.P. Sheng, H.Q. Yu, X.Y. Li, Extracellular polymeric substances (EPS) of microbial aggregates in biological wastewater treatment systems: a review, *Biotechnol. Adv.*, 28 (2010) 882–894.
- [14] S. Saminathan, H. Liu, T.V. Nguyen, S. Vigneswaran, Organic matter removal from biologically treated sewage effluent by flocculation and oxidation coupled with flocculation, *Desal. Wat. Treat.*, 32 (2011) 133–137.
- [15] X.D. Ruan, L. Li, J.X. Liu, Flocculating characteristic of activated sludge flocs: Interaction between Al^{3+} and extracellular polymeric substances, *J. Environ. Sci.*, 25 (2013) 916–924.
- [16] I. Nopens, N. Nere, P.A. Vanrolleghem, D. Ramkrishna, Solving the inverse problem for aggregation in activated sludge flocculation using a population balance framework, *Water Sci. Technol.*, 56 (2007) 95–103.
- [17] E. Torfs, G. Bellandi, I. Nopens, Towards mechanistic models for activated sludge flocculation under different conditions based on inverse problems, *Water Sci. Technol.*, 65 (2012) 1946–1953.
- [18] E. Torfs, A. Dutta, I. Nopens, Investigating kernel structures for Ca-induced activated sludge aggregation using an inverse problem methodology, *Chem. Eng. Sci.*, 70 (2012) 176–187.

- [19] F. Mietta, C. Chassagne, R. Verney, J.C. Winterwerp, On the behavior of mud floc size distribution: model calibration and model behavior, *Ocean Dyn.*, 61 (2011) 257–271.
- [20] J. Bridgeman, B. Jefferson, S. Parsons, Computational fluid dynamics modelling of flocculation in water treatment: a review, *Eng. Appl. Comp. Fluid Mech.*, 3 (2009) 220–241.
- [21] A.M. Karpinska, J. Bridgeman, CFD-aided modelling of activated sludge systems – a critical review, *Water Res.*, 88 (2015) 861–879.
- [22] D.H. Li, J. Ganczarzyk, Fractal geometry of particle aggregates generated in water and waste-water treatment processes, *Environ. Sci. Technol.*, 23 (1989) 1385–1389.
- [23] Z.L. Li, D.J. Zhang, P.L. Lu, S.W. Zeng, Y.H. Yang, Factors of effecting on floc size distribution and fractal dimension of activated sludge, *Environ. Sci.*, 34 (2013) 1975–3980.
- [24] D. Ramkrishna, *Population Balances: Theory and Applications to Particulate Systems in Engineering*, Academic Press, London, UK, 2000.
- [25] I. Nopens, P.A. Vanrolleghem, D. Beheydt, Comparison and pitfalls of different discretised solution methods for population balance models: a simulation study, *Comput. Chem. Eng.*, 29 (2005) 367–377.
- [26] S. Kumar, D. Ramkrishna, On the solution of population balance equations by discretization—I. A fixed pivot technique, *Chem. Eng. Sci.*, 51 (1996) 1311–1332.
- [27] P. Spicer, S. Pratsinis, Coagulation and fragmentation: universal steady-state particle-size distribution, *AIChE J.*, 42 (1996) 1612–1620.
- [28] T. Serra, X. Casamitjana, Modelling the aggregation and break-up of fractal aggregates in a shear flow, *Appl. Sci. Res.*, 59 (1998) 255–268.
- [29] J. Flesch, P. Spicer, S. Pratsinis, Laminar and turbulent shear-induced flocculation of fractal aggregates, *AIChE J.*, 45 (1999) 1114–1124.
- [30] F. Maggi, F. Mietta, J.C. Winterwerp, Effect of variable fractal dimension on the floc size distribution of suspended cohesive sediment, *J. Hydrol.*, 343 (2007) 43–55.
- [31] Z.L. Li, P.L. Lu, D.J. Zhang, G.C. Chen, S.W. Zeng, Q. He, Population balance modeling of activated sludge flocculation: investigating the influence of extracellular polymeric substances (EPS) content and zeta potential on flocculation dynamics, *Sep. Purif. Technol.*, 16 (2016) 91–100.
- [32] I. Nopens, T. Koegst, K. Mahieu, P.A. Vanrolleghem, PBM and activated sludge flocculation: from experimental data to calibrated model, *AIChE J.*, 51 (2005) 1548–1557.
- [33] F. Maggi, *Flocculation Dynamics of Cohesive Sediment*, PhD Thesis, Delft University of Technology, Delft, 2005.
- [34] K. Kusters, J. Wijers, D. Thoenes, Aggregation kinetics of small particles in agitated vessels, *Chem. Eng. Sci.*, 52 (1997) 107–121.
- [35] Y. Sang, P. Englezos, Flocculation of precipitated calcium carbonate (PCC) by cationic tapioca starch with different charge densities. II: Population balance modeling, *Colloids Surf., A*, 414 (2012) 520–526.